# Infrared spectrum analysis method for detection and early warning of longitudinal tear of mine conveyor belt

Yang, Ruiyun; Qiao, Tiezhu; Pang, Yusong; Yang, Yi; Zhang, Haitao; Yan, Gaowei

**DOI**
10.1016/j.measurement.2020.107856

**Publication date**
2020

**Document Version**
Accepted author manuscript

**Published in**
Measurement: Journal of the International Measurement Confederation

**Citation (APA)**
Yang, R., Qiao, T., Pang, Y., Yang, Y., Zhang, H., & Yan, G. (2020). Infrared spectrum analysis method for detection and early warning of longitudinal tear of mine conveyor belt. *Measurement: Journal of the International Measurement Confederation*, *165*, Article 107856. https://doi.org/10.1016/j.measurement.2020.107856

# Infrared Spectrum Analysis Method for Detection and Early Warning of Longitudinal Tear of Mine Conveyor Belt

**Ruiyun Yang[a,c] , Tiezhu Qiao[*a,c] , Yusong Pang[b] , Yi Yang[a,c] , Haitao Zhang[a,c] , Gaowei Yan[d]**

[a]Key Laboratory of Advanced Transducers and Intelligent Control System, Ministry of Education, Taiyuan University of Technology, Taiyuan 030024, China

[b]Section of Transport Engineering and Logistic, Faculty of Mechanical, Maritime and Materials Engineering, Delft University of Technology, 2628 CD Delft, Netherlands

[c]College of Physics and Optoelectronics, Taiyuan University of Technology, Taiyuan 030024, China

[d]College of Electrical and Power Engineering, Taiyuan University of Technology, Taiyuan 030024, China

## Highlights

1) Monitor longitudinal tear with infrared thermography

2) Overcome the interference caused by the change of infrared image threshold

3) Select the appropriate detection spectral passband

4) Coefficient T can be used to quantitatively describe tear change characteristics

**Abstract:** A novel approach based on infrared spectrum analysis for early-warning of longitudinal tearing of the conveyor belt was proposed in the paper. Unlike most existing methods, the proposed method monitors the change process of the infrared radiation field of the longitudinal tearing through the infrared thermal imaging technology, and judges whether there is the risk of the longitudinal tearing of the conveyor belt through the frequency-domain characteristic coefficient T of the infrared radiation field. Experimental results exhibit that the characteristic coefficient T can quantitatively describe the change characteristics of infrared radiation field during the tearing process of conveyor belt. When the conveyor belt is complete penetration, the T value fluctuates violently from 0.6 to 1.6.

This characteristic can be used as the precursor information of the tearing process, which broadens the train of thought for identification and early warning of conveyor belt longitudinal tearing.

**Keywords: longitudinal tearing; infrared spectrum analysis detection (ISAD); fast fourier transform; frequency domain characteristics**

## 1. Introduction

Belt conveyor [1] has high transportation efficiency and strong conveying capacity. It is a long-distance continuous conveyor commonly used in coal mines. Conveyor belt is the most important part of belt conveyor. Longitudinal tearing of conveyor belt mainly occurs at loading points of belt conveyor, such as the outlet of loading trough or funnel and the discharge outlet of belt conveyor. In mining operations, because of the complex working environment of the mine, sharp metal impurities such as bolts and anchor cables are often mixed in the coal [2], which may scratch or penetrate the belt at loading and unloading points, thus causing longitudinal tearing. Compared with other problems in conveyor belt transportation, such as transverse tearing of conveyor belt, the damage of longitudinal tearing is greater, and even leads to the shutdown of the whole mining process, leading to huge economic losses to industrial enterprises [3]. To detect the longitudinal tear of the conveyor belt, various methods and systems are proposed in literature [4-12].The traditional methods of conveyor belt longitudinal tear detection at home and abroad mainly include X-ray detection [13,14] and machine vision detections. In 2011, Rong et al. [15] used X-ray detection method to detect tear of strong conveyor belt. This method is intuitive, reliable and has good detection effect, but it is not suitable for non-steel core conveyor belt, and the physical hazards to operators caused by long-term use are not taken into account. With the rapid development of computer technology, machine vision technology has been gradually applied to the fault diagnosis of belt conveyor. Since 2006, Qi et al. [16-18] combined with Labview platform, applied machine vision technology to the longitudinal tear detection of belt conveyor. In 2018, Wang et al. [19] proposed a visual detection method for belt tear, which combines visible binocular vision and laser line source. This method is susceptible to light intensity change and dust smoke interference in the process of image acquisition, which has an impact on subsequent image processing, and can only recognize complete tear, without tear warning ability.In order to solve the problem of visible light detection, researchers have designed several methods related to infrared detection of longitudinal tear. Zhao [20]

proposed a method of belt longitudinal tear detection based on support vector machine infrared image segmentation.Qiao and Liu [21] designed a real-time visible and infrared vision detection system for longitudinal tear of conveyor belt. Qiao and Chen [22] proposed a comprehensive binocular vision detection method based on the fusion of visible and infrared vision,which overcomes the problem of poor visibility in underground.The above-mentioned methods capture image by infrared camera and detect the belt tear based on a histogram of the infrared image and a fixed threshold. However, the threshold is subject to change due to factors such as the work environment and runtime, resulting in poor universality of the methods [23].

Infrared thermal image is a contrast image reflecting the intensity of infrared thermal radiation. Any object whose temperature is higher than absolute zero will radiate infrared rays. Infrared thermal radiation has strong characteristics of penetrating dust. In 2013, Zhang [24] realized on-line detection of insulator fault of high-voltage transmission line by using infrared thermal imaging method. In 2016, Zou and Luo [25] carried out theoretical analysis and experimental verification by using infrared thermal image to analyze the crack damage of tunnel surrounding rock under blasting action. In 2017, Yuan et al.[26] realized the detection of surface crack of impact damage of carbon fiber laminate using infrared thermal image. It can be seen that infrared thermal radiation image has the characteristics of realizing on-line non-contact detection and feature image is more intuitive.It can be applied to fault detection of various field equipment as well as defect and corrosion detection of various materials [27,28]. It is very suitable for on-line detection of non-metallic materials with poor thermal conductivity, such as longitudinal tear of conveyor belt. Different from infrared camera relying on fixed threshold,this method relies on the change of thermal radiation spectrum for detection, which can effectively solve the problem of interference accuracy of infrared image threshold change and achieve the purpose of tear early warning. Based on this characteristic of infrared thermal image, In 2017, Zhu [29] put forward a design concept of infrared thermal image detection system for conveyor belt tear. It is worth noting that no one has designed a specific realization method to detect the longitudinal tear of conveyor belt with infrared thermal image until now.

Therefore, this paper presents a specific realization method to detect the longitudinal tear of conveyor belt with infrared thermal image. As mentioned in the first paragraph, when sharp metal foreign matters mixed with coals like bolts are blocked at the discharge port, they may move with contact and extrusion with rough conveyor belts, which will produce severe friction and heat. The heat flow generated will concentrated in the contact area and diffuse to the surrounding area with low temperature through the contact point, forming a frictional temperature field. Under the shearing action of the metal foreign body and the conveyor belt, it is easy to penetrate into the conveyor belt, thus forming the

sticking motion of the belt, and eventually causing the longitudinal tear of the conveyor belt [30.31] , as shown in Fig. 1. In order to study the process of longitudinal tearing of conveyor belt, realize the early warning ability of longitudinal tearing, and improve the reliability and safety of conveyor belt on coal mine belt conveyor, this method focuses on the stage from friction to pierce between sharp metal foreign matters and belt, The method captures the infrared thermal image through the infrared thermal imager installed on the lower surface of the conveyor belt at the discharge port, extracts temperature values of different pixels in the thermal image by software, and uses the software of MATLAB to fit thermal radiation emittance curve according to the temperature values of different pixels and analyze the thermal radiation features of target friction heating and the radiation characteristics of background. Innovatively, the infrared radiation difference in the tearing stage of the conveyor belt is used to select the appropriate spectral passband to obtain the maximum target background radiation contrast [32]. The radiation emittance values of different pixels on the selected spectral passband are extracted to monitor the change of the infrared radiation field when the conveyor belt is torn. The FFT technology, which is widely used in image processing field, is innovatively applied to infrared radiation field matrix to obtain two-dimensional spectrum signal of infrared radiation field. By calculating the mean square deviation of two-dimensional spectrum signal of infrared radiation field, the quantitative index describing the evolution characteristics of infrared radiation field in frequency domain, i.e. the characteristic coefficient T of infrared radiation field in frequency domain, is obtained. Taking radiation field as the carrier of tearing and symptom information detection, accurate information of tearing and symptom is obtained through carrier information detection and demodulation, and defect detection and early warning are made. The principle is shown in Fig. 2.

The remainder of the paper organization is shown as follows: The Section 2 introduces the infrared spectrum analysis method. The Section 3 provides experiment and analysis. The Section 4 gives the overall conclusion.

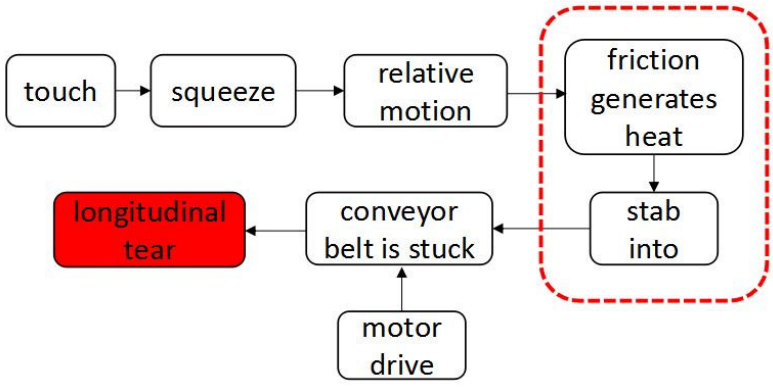


**Fig.1. Diagram of longitudinal tearing development process**

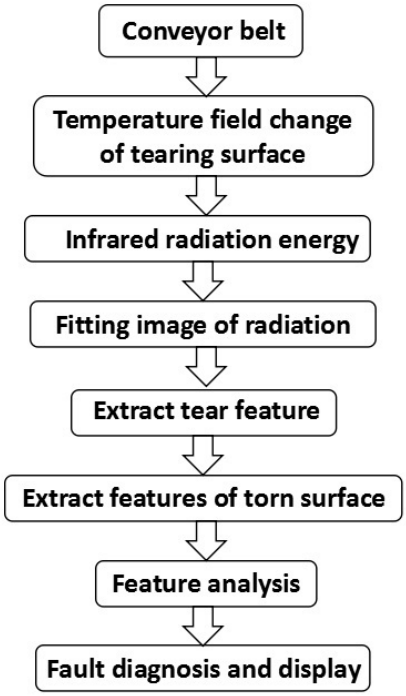


**Fig.2 Infrared detection schematic diagram**

## 2. The ISAD method

Infrared spectrum analysis methods mainly include spectral band selection, spectral radiation fitting and spectral feature extraction and analysis.Firstly, in order to obtain the maximum contrast between the target of friction heat generation and the background , it is necessary to select the appropriate spectral passband [33] by analyzing the spectral distribution of thermal radiation.Secondly, the radiation fitting image of selected spectral passband is obtained by or using MATLAB to process the temperature matrix of thermal image [34]. Thirdly, two-dimensional spectrum signal of infrared radiation field is obtained by fast Fourier transform. All details are described in the following sections.

### 2.1 Spectral passband selection

All objects above absolute zero temperature emit infrared radiation to surrounding areas continuously. The infrared radiation emitted by the conveyor belt in normal operation is basically the same. The friction between the metal foreign matters and the surface of the conveyor belt will produce a lot of heat, accompanied by thermal radiation energy. Infrared detection technology is sensitive to infrared thermal radiation, so it can effectively detect the thermal radiation change of conveyor belt and obtain the distribution rule of thermal radiation by establishing an ideal black body model, Planck's formula [35] reveals the basic law of infrared radiation spectrum of blackbody, as follows:

$$M = \frac{2\pi hc^2}{\lambda^5[e^{(hc/\lambda bT)} - 1]} = \frac{c_1}{\lambda^5[(e^{c_2/\lambda T} - 1)]} \qquad (1)$$

In the formula (1), M is the spectral radiation emittance of the blackbody; $\lambda$ is the wavelength, whose unit is m; $c = 3 \times 10^8 m/s$ is the speed of light; $c_1$ and $c_2$ is respectively called the first radiation constant and the second radiation constant; $h = 6.634 \times 10^{-34} J \cdot s$ is Planck constant; $b = 1.38054 \times 10^{-23} J/K$ is Boltzmann constant; T is the absolute temperature of the blackbody, whose unit is K.

Fig. 3 simulates the curve of blackbody infrared radiation emittance varying with wavelength between ambient temperature 300K and rubber temperature 400K when conveyor belt is tearing, and the position of maximum value of each curve has been marked. It can be seen from the figure that the radiation intensity of blackbody varies continuously with the change of wavelength at different temperatures. In order to maximize the contrast between the target and the background of friction heating, the practical work is to select the appropriate working wavelength so as to make the change rate of spectral radiation with temperature reach the maximum.

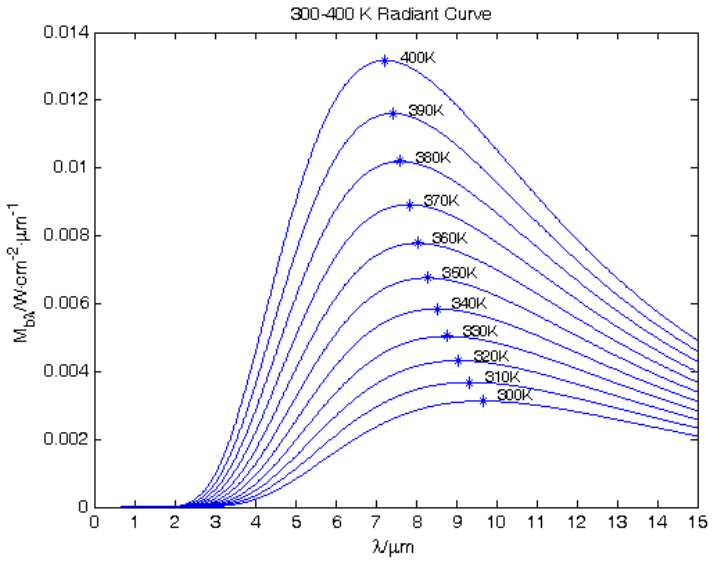


**Fig.3. Spectral Distribution of Blackbody Radiation Emissivity**

Through the derivation of the Planck radiation formula and the accurate solution of the computer numerical solution, the following results are obtained:

$$\lambda_M = 2410/T(\mu m) \qquad (2)$$

That is to say, the maximum value of spectral radiation contrast exists at $\lambda_M = 2410/T(\mu m)$. Formula (2) expresses concisely that if we want to obtain the maximum spectral contrast for the target with temperature of T, we should choose the

nearby spectral band as the working band of the infrared system.

When the conveyor belt is working normally, the temperature is about 300K, and the rubber radiation coefficient is $\varepsilon = 0.95$. Assuming the transmission transmissivity is $\tau = 0.66$ at a certain distance , the radiation temperature transfer from the target to the imaging system is:

$$\mathrm{T}' = \frac{c_2 \mathrm{T}}{c_2 - \lambda \mathrm{T} \ln(\tau\varepsilon)} = 278K \qquad (3)$$

Where $\mathrm{c}_2 = 14388(\mu \mathrm{n}.K)$ is the second Planck constant and $\lambda \mathrm{T} = 2938(\mu \mathrm{m}.K)$ is the Wien displacement law. $\mathrm{T}' = 278$ is substituted into formula (2) to get

$$\lambda_{\mathrm{M}} = \frac{2410}{\mathrm{T}'} = 8.67(\mu \mathrm{m}) \qquad (4)$$

When tearing occurs, the temperature of the rubber material of the conveyor belt is about 400k, and its surface radiation coefficient is $\varepsilon = 0.95$ , the transmission transmissivity is $\tau = 0.66$:

$$\mathrm{T}' = \frac{c_2 \mathrm{T}}{c_2 - \lambda \mathrm{T} \ln(\tau\varepsilon)} = 371K \qquad (5)$$

$\mathrm{T}' = 371$ is substituted into formula (2) to get

$$\lambda_{\mathrm{M}} = \frac{2410}{\mathrm{T}'} = 6.50(\mu \mathrm{m}) \qquad (6)$$

From the above formulas, it is concluded that the working band of $6 \sim 9 \mu m$ is suitable.

## 2.2 Spectral radiation fitting

Infrared thermal image of conveyor belt tearing process is collected by infrared thermal imager and imported into the software to process the data. Thereby, a set of temperature data of target and background are obtained and saved in matrix form, and then the temperature data of the image are fitted with the spectral radiation curve of MATLAB. Finally, the temperature data of the thermal image is transformed into the $6 \sim 9 \mu m$ infrared radiation field matrix of the band.

After we get the thermal images of the target captured by the infrared thermal imager, we import them into the thermal image analysis software of the thermal imager for extracting the temperature values of all pixels. These data can be saved in the form of a matrix to achieve universal processing. Table 1 is a screenshot of a part of the pixel thermometer derived by the software.

**Table 1: Derived pixel temperature data for target thermal images**

| | EP | EQ | ER | ES | ET | EU | EV | EW | EX | EY |
|---|---|---|---|---|---|---|---|---|---|---|
| 106 | 50 | 51.4 | 51.4 | 51.5 | 51.6 | 51.1 | 50.2 | 49 | 47.6 | 46.1 |
| 107 | 53.3 | 56.4 | 54.2 | 52.3 | 51.6 | 51 | 50.2 | 49 | 47.6 | 46.1 |
| 108 | 56.3 | 61 | 58 | 53.3 | 51.7 | 51 | 50.2 | 49 | 47.5 | 46 |
| 109 | 56.9 | 61 | 60.1 | 54.2 | 51.8 | 50.9 | 50.1 | 48.9 | 47.5 | 45.9 |
| 110 | 57.5 | 61.2 | 61 | 54.8 | 51.8 | 50.8 | 50 | 48.8 | 47.4 | 45.9 |
| 111 | 58.2 | 62.9 | 61.8 | 55.1 | 51.7 | 50.6 | 49.7 | 48.7 | 47.2 | 45.7 |
| 112 | 58.2 | 63.8 | 62.3 | 55.2 | 51.6 | 50.4 | 49.5 | 48.3 | 47 | 45.6 |
| 113 | 58.7 | 64.2 | 62.6 | 55.3 | 51.4 | 50.2 | 49.3 | 48.2 | 46.8 | 45.4 |
| 114 | 58.6 | 64.2 | 62.6 | 55.2 | 51.2 | 49.9 | 49.1 | 48 | 46.6 | 45.2 |
| 115 | 57.4 | 62.6 | 61.7 | 54.9 | 50.8 | 49.6 | 48.8 | 47.7 | 46.4 | 45 |
| 116 | 56.2 | 61.2 | 60.8 | 54.5 | 50.5 | 49.2 | 48.5 | 47.4 | 46.2 | 44.9 |
| 117 | 55.3 | 60.6 | 60.2 | 54 | 50 | 48.8 | 48.1 | 47.1 | 45.9 | 44.6 |
| 118 | 54 | 59.6 | 59.2 | 53.2 | 49.5 | 48.4 | 47.7 | 46.8 | 45.6 | 44.4 |
| 119 | 52.1 | 57.4 | 57.3 | 51.9 | 48.8 | 47.9 | 47.3 | 46.4 | 45.2 | 44 |
| 120 | 50.4 | 54.6 | 54.6 | 50.5 | 48.1 | 47.3 | 46.8 | 45.9 | 44.9 | 43.7 |
| 121 | 48 | 51.5 | 51.8 | 49.2 | 47.4 | 46.9 | 46.3 | 45.5 | 44.5 | 43.2 |
| 122 | 46.3 | 48.6 | 49.1 | 47.5 | 46.7 | 46.3 | 45.8 | 45 | 44 | 42.9 |
| 123 | 44.9 | 46.4 | 46.9 | 46.4 | 46 | 45.7 | 45.3 | 44.5 | 43.6 | 42.4 |
| 124 | 44.1 | 44.9 | 45.5 | 45.4 | 45.3 | 45.1 | 44.6 | 44 | 43.1 | 42.1 |
| 125 | 43.6 | 44.1 | 44.5 | 44.6 | 44.7 | 44.5 | 44 | 43.4 | 42.5 | 41.6 |
| 126 | 43 | 43.5 | 43.8 | 44 | 44.1 | 43.9 | 43.5 | 42.9 | 42.1 | 41.2 |
| 127 | 42.5 | 42.9 | 43.2 | 43.4 | 43.4 | 43.2 | 42.8 | 42.3 | 41.6 | 40.7 |
| 128 | 42 | 42.4 | 42.7 | 42.8 | 42.8 | 42.6 | 42.3 | 41.7 | 41 | 40.3 |
| 129 | 41.4 | 41.8 | 42.1 | 42.1 | 42.1 | 41.9 | 41.7 | 41.1 | 40.5 | 39.8 |
| 130 | 40.9 | 41.2 | 41.4 | 41.5 | 41.5 | 41.4 | 41 | 40.6 | 40 | 39.3 |
| 131 | 40.3 | 40.6 | 40.9 | 40.9 | 41 | 40.7 | 40.4 | 40 | 39.4 | 38.8 |
| 132 | 39.7 | 40 | 40.2 | 40.3 | 40.3 | 40.1 | 39.9 | 39.5 | 38.9 | 38.3 |
| 133 | 39.2 | 39.5 | 39.7 | 39.8 | 39.7 | 39.5 | 39.2 | 38.9 | 38.4 | 37.8 |

The processing of the temperature matrix belongs to the space domain method. The resolution of the thermal imager is 320 * 240. The data input model M (x, y) represents the temperature matrix of the infrared thermal image. Here, the interval of X is set as [1, 320], and the interval of Y is set as [1,240]. Because the research is dynamic real-time processing, it is necessary to transform these discrete quantities into the corresponding values of continuous coordinates for real-time processing, which can be expressed as (x, y) = (1, 1) (320,240). Formula (7) is a temperature matrix represented by a two-dimensional array.

$$\mathrm{M}(x,y)=\begin{Bmatrix} m(1,1) & m(1,2) & \cdots & \cdots & m(1,240) \\ m(2,1) & m(2,2) & \cdots & \cdots & m(2,240) \\ \cdots & \cdots & \cdots & \cdots & \cdots \\ \cdots & \cdots & \cdots & \cdots & \cdots \\ m(320,1) & \cdots & \cdots & \cdots & m(320,240) \end{Bmatrix} \tag{7}$$

At the same band and at different temperatures, the radiation emissivity M value of different pixels can be extracted by software. Because the resolution of the thermal imager is 320*240, that is, the thermal image has 320*240=76800 pixels, there are 76800 thermal radiation curves at different temperatures. Therefore, we can get the emittance m value of all pixels in 6-9 um band by integration.

From Planck's spectral radiation formula (1), we can see that the spectral radiation of blackbody $\mathrm{M}(\lambda,T)$ has the following relationship with wavelength $\lambda$ and temperature T.

$$\mathrm{M}=\frac{2\pi hc^2}{\lambda^5[e^{(hc/\lambda bT)}-1]}=\frac{c_1}{\lambda^5[(e^{c_2/\lambda T}-1)]} \qquad (1)$$

The spectral integral of $\mathrm{M}(\lambda,T)$ in the band $\Delta\lambda=\lambda_1\sim\lambda_2$ is called band radiosity.

$$\mathrm{M}(\Delta\lambda,T)=\int_{\lambda_1}^{\lambda_2}\mathrm{M}(\lambda,T)d\lambda \qquad (8)$$

In formula (8), let $\lambda_1=6,\lambda_2=9$, the matrix of infrared radiation field in $6\sim9\mu m$ band can be calculated by or using the rectangular integral method of MATLAB.

## 2.3 Spectrum feature extraction and analysis

Quantitative extraction of image features means processing and analyzing the input information contained in the image, and extracting the information which is not easily disturbed by random factors as feature parameters. Feature extraction process is a process of removing redundant information, which can improve the recognition accuracy, reduce the amount of calculation and improve the speed of operation. Infrared radiation field data is a special type of data. Its infrared radiation value represents the distribution rule of infrared radiation with time and space. When metal foreign matters penetrate the defective area, its radiation strengthens with the increasing friction temperature. Infrared image of conveyor belt mainly reflects the change of radiation amount of pixels, and different penetration degree has different infrared radiation characteristics, which can be described by characteristic quantity.

For infrared radiation image, the image itself contains periodic, aperiodic and noise information in the space domain. It is very difficult to extract infrared radiation thermal image in the space domain. The infrared radiation image is processed in complex frequency domain using FFT technology. Parameters that can describe the infrared radiation tearing characteristics in spatial domain are found according to the change of image radiation characteristics. For two-dimensional FFT of image, an infrared radiation field image of 6-9 micron band composed of M*N pixels is represented by f(x, y), where x = 1,2,... M; y = 1,2,... N; In formula (9), F (u, v) is the spectrum obtained by f(x, y) two-dimensional FFT

$$\mathrm{F(u,v)}=\sum_{x=1}^{M}\sum_{y=1}^{N}f(x,y)e^{-j2\pi(\frac{ux}{M}+\frac{vy}{N})} \qquad (9)$$

Where u= 1,2,…,M； v =1,2,…,N

The spatial domain image f (x, y) can be converted to the spectral image F (u, v) by two-dimensional FFT, and the thermal image can be shifted its frequency to make the point of F (u, v) image locate in the image center. For two-dimensional FFT spectral images, the brightness of the original frequency domain image is moved to the center of the image after shifting frequency represents the high-frequency component of space, that is, the larger the gradient value and the more the bright part, the more intensively the space thermal image radiation changes; the dark around the image represents the low frequency component of space domain image, that is, the smaller the gradient and the

more the dark part , the space radiation changes. In order to increase the spectral contrast of two-dimensional FFT, logarithmic transform is used to process the spectrum and enlarge the high-frequency part of the image. The infrared radiation thermal image before and after two-dimensional FFT is shown in Fig. 4.

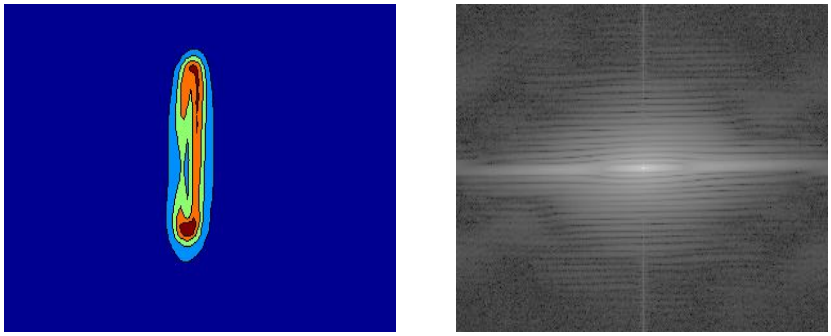

（a）Thermal image before 2D FFT　　（b）Thermal image after 2D FFT

**Fig.4. Infrared radiation thermal images before and after two-dimensional Fast Fourier Transform**

Assuming that the spectrum of infrared radiation thermal image obtained by two-dimensional FFT is $F_t(\mathrm{u},\mathrm{v})$at time t , the spectrum of $F_t{}'(\mathrm{u},\mathrm{v})$image with bright center is obtained after shifting frequency of $F_t(\mathrm{u},\mathrm{v})$ image. Then the contrast between high frequency region and low frequency region is enhanced by logarithmic transformation for $F_t{}'(\mathrm{u},\mathrm{v})$ image to obtain image $F_t{}''(\mathrm{u},\mathrm{v})$.The specific transformation method is shown in formula (10-12).The more highlights in the spectrum, the larger the radiation value (height) at the center of the spectrum is, and the more discrete the spatial characteristics of the spectrum are. According to this characteristic of the spectrum, the dispersion degree of the spectrum can be calculated effectively by means of mean square deviation of eigenvalues, so that the change rule of the infrared radiation characteristics of the surface under the conveyor belt during tearing can be qualitatively described. The mean square deviation of $F_t{}''(\mathrm{u},\mathrm{v})$is calculated by std2 function of MATLAB to describe the characteristic coefficient T of infrared radiation field in frequency domain, which is a quantitative index describing the evolution characteristics of infrared radiation field in frequency domain.

$$F_t(\mathrm{u},\mathrm{v}) = \mathrm{fft2}[\mathrm{f}(\mathrm{x},\mathrm{y})] \qquad (10)$$

$$F_t{}'(\mathrm{u},\mathrm{v}) = \mathrm{fftshift}[F_t(\mathrm{u},\mathrm{v})] \qquad (11)$$

$$F_t{}''(\mathrm{u},\mathrm{v}) = \log\{\mathrm{abs}[F_t{}'(\mathrm{u},\mathrm{v})]\} \qquad (12)$$

Characteristic parameters used in this paper:

(1) Mean value E of amplitude spectrum in frequency domain: it refers to the average

number of radiation values of each point in the sampling area. When tearing occurs, the temperature rises abnormally and the radiation value is large. The calculation formula is shown in formula (13):

$$\mathrm{E} = \frac{\sum_{U=1}^{M}\sum_{V=1}^{N} F_t''(\mathrm{u,v})}{MN} \qquad (13)$$

(2) Frequency domain amplitude spectrum mean square deviation T: it refers to the amount of radiation value dispersion degree on both sides of the radiation mean. If the radiation values of each point in the sampling area are relatively close, the radiation mean square deviation is small. This parameter reflects whether the radiation is uniform. The calculation formula is shown in formula (14):

$$\mathrm{T} = \{\sum_{U=1}^{M}\sum_{V=1}^{N}[F_t''(\mathrm{u,v}) - \mathrm{E}]^2\}^{\frac{1}{2}} \qquad (14)$$

## 3. Experiments and analysis

An experimental platform was built in the laboratory to verify the infrared spectrum analysis and detection method proposed in this paper. The experimental device, process and results are as follows:

### 3.1 Experimental device

The conveyor belt longitudinal tear detection experimental platform is shown in Fig. 5. The conveyor adopted in the experiment shown in Fig. 6 is the conventional through belt conveyor used in underground. The width of conveyor belt is 0.8 m,thickness is 19 mm, longitudinal tensile strength is 1250 N/mm, wear rate is less than 90 mm3/(N • m), The temperature of the working environment is 25°C and the maximum operating temperature of conveyor belt is 40°C which is close to the actual mining conveyor belt. The steel chisel is fixed above the conveyor belt to simulate the hazard.The steel chisel can rub against conveyor belt and then penetrate the conveyor belt to cause longitudinal tear.Flir A300 infrared thermal imager is used to capture infrared thermal images. The temperature measurement range is 0-350°C, the accuracy is ± 2°C or ± 2% of displaying data, the working wavelength is 7.5-13 um, and the spatial resolution is 1.36 mrad.The infrared thermal imager is installed under the belt to capture the infrared thermal image whose resolution is 320*240.Infrared thermal image data is transmitted to PC through Ethernet, CPU is i7-9750h, memory is 16GByte and 512GB-SSD. The temperature matrix data files are extracted by processing the infrared thermal image with the software of the thermal imager on the PC, and the frequency-domain characteristic coefficient T of the damage characteristics of the conveyor belt is processed based on based on Win10, MATLAB R2014a and VS(Microsoft Visual Studio).This experiment was repeated three times.

### 3.2 Experimental process

(1) There is only one conveyor belt in the laboratory and the cost is high. Therefore, this experiment needs to be completed without tearing the whole conveyor belt. A grinder is used to grind the surface of conveyor belt in static state. Because the process of heat generation by friction is the same as that of heat generation by friction between metal foreign bodies and conveyor belt in running state, a grinder is used to simulate the process of heat generation by friction between metal foreign bodies and conveyor belt. The infrared thermal imager is positioned on the lower surface of the conveyor belt, and the thermal radiation from the puncture of the upper surface to the lower surface is collected (Fig. 5, 6). The sampling amplitude per second is set to 5.

(2) At the beginning of the experiment, infrared thermal imager collects infrared thermal radiation imaging of conveyor belt under normal condition for a while; and opens metal cutting machine to grind the surface of conveyor belt, and the thermal imager records the change of thermal radiation distribution on the surface of conveyor belt with the penetration depth of metal; then stops and moves out of metal cutting machine. Record the exothermic process of leaving the metal foreign body after forming the penetration point. Then we continue to open the metal cutting machine to grind the penetration point, and record the thermal radiation distribution of metal penetrating the conveyor belt; then we stop grinding and remove the metal cutting machine, record the heat dissipation process of the conveyor belt at the crack after complete puncture.

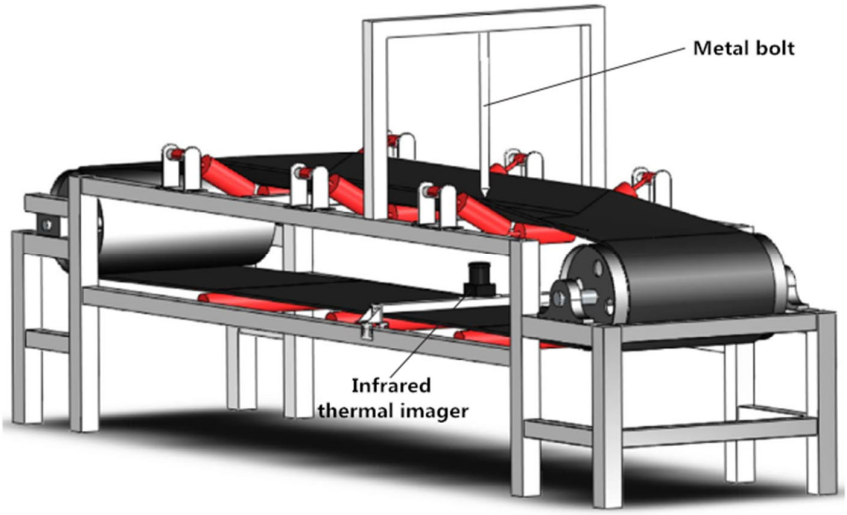


**Fig.5. Installation position diagram of infrared thermal imager**

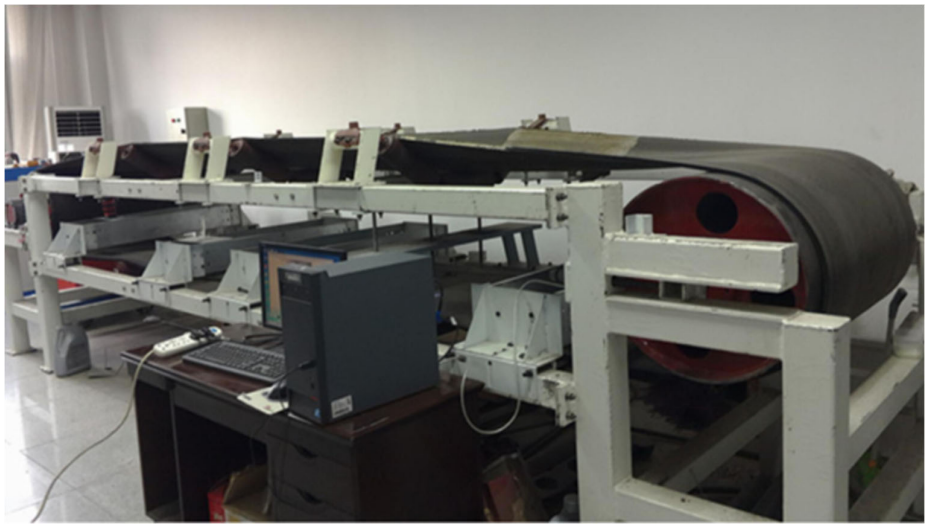

**Fig.6.The experiment platform of the ISAD method**

### 3.3 Experimental results

We use infrared thermal imager to collect thermal images of conveyor belt targets in tearing process, records the whole process of tearing [36-38]. With the increasing depths of sharp metal foreign bodies piercing belt (as shown in Fig. 7), the temperature distribution of each stage in the tearing area is obtained (as shown in Fig. 8 (a)(b)(c)).

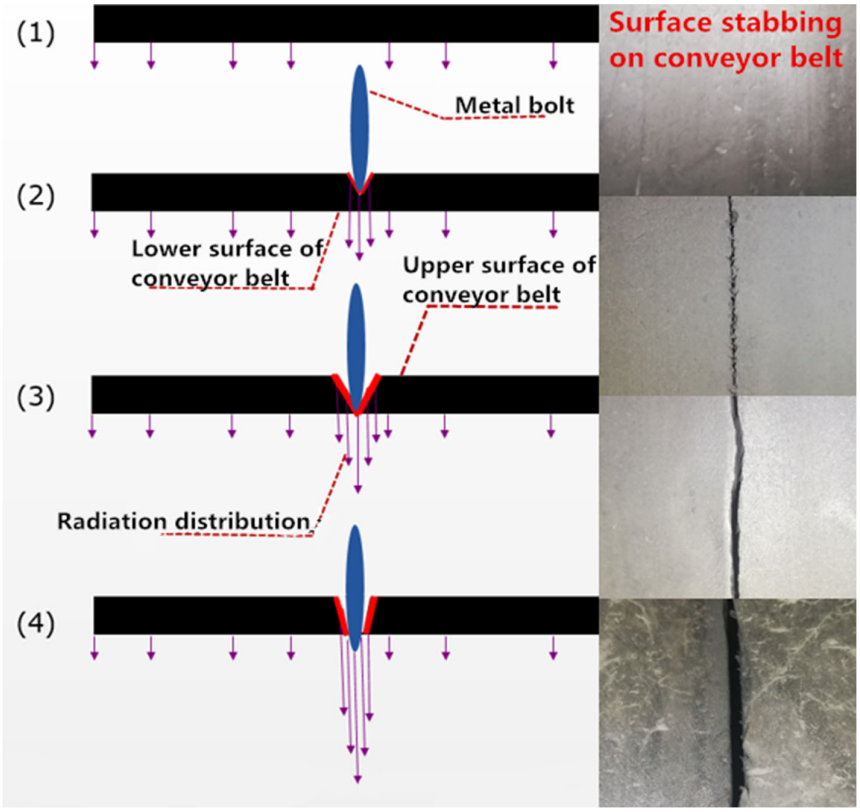

(1) normal state (2) penetration point (3) penetration deeper (4) complete penetration

**Fig.7. Diagram of friction penetration process of bolt**

Using the rectangular numerical integration of MATLAB, the radiance of the image temperature matrix derived from the thermal imager can be calculated in the band of 6-9 um (as shown in Fig.8(d)(E)(f)). Through two-dimensional FFT, frequency shift processing and logarithmic transformation, the processed spectrum is obtained. It can be found that the bright part in the center of the spectrum will increase with the friction experiment of sharp metal foreign bodies, that is, the high frequency part in the corresponding space domain image will increase, which indicates that the radiation difference caused by the temperature of the image is more obvious, and the transition boundary between the high radiation region and the low radiation region is short, The radiation separation phenomenon of radiation field is obvious, and the change trend of spectrum is shown in Fig. 8(g) (H) (I).

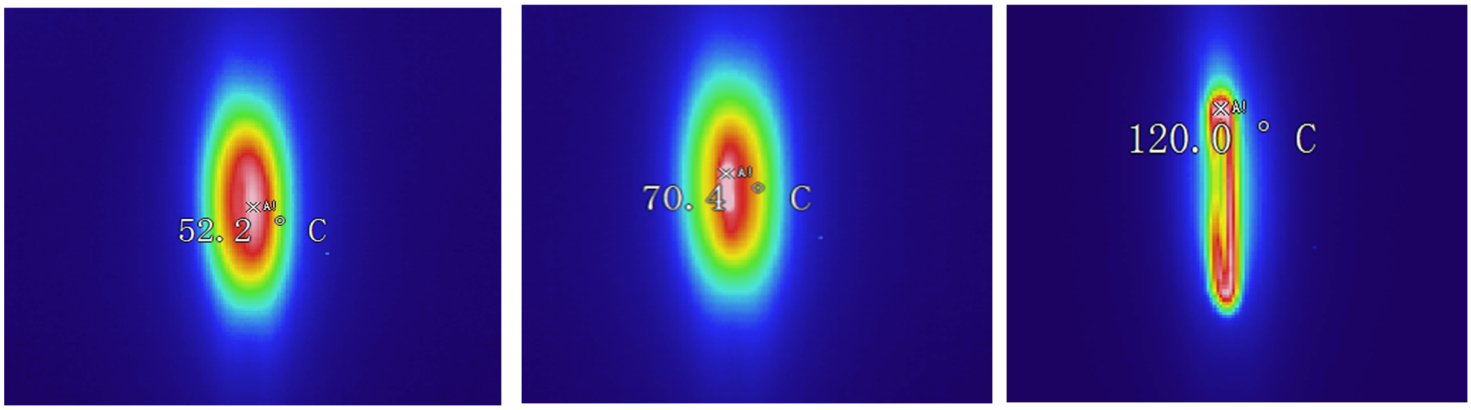


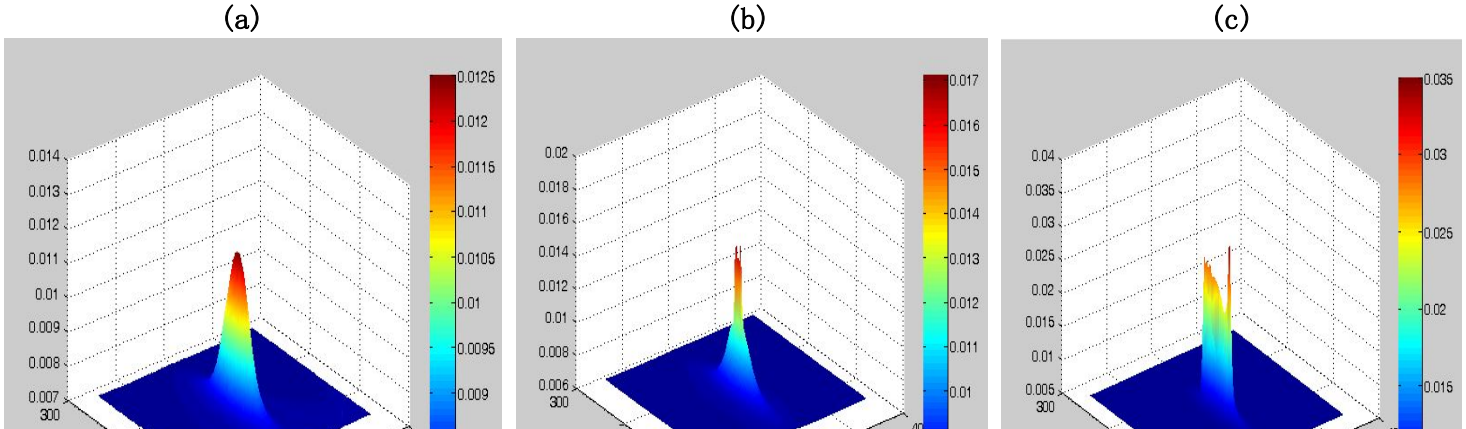

(d) (e) (f)

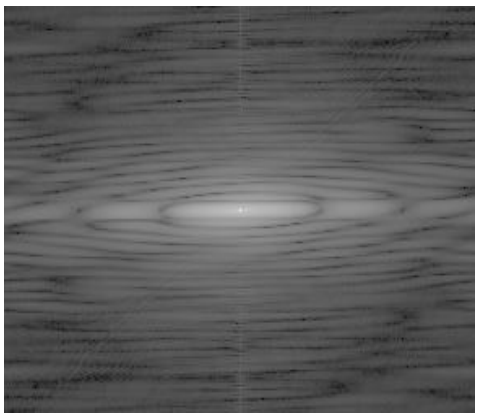

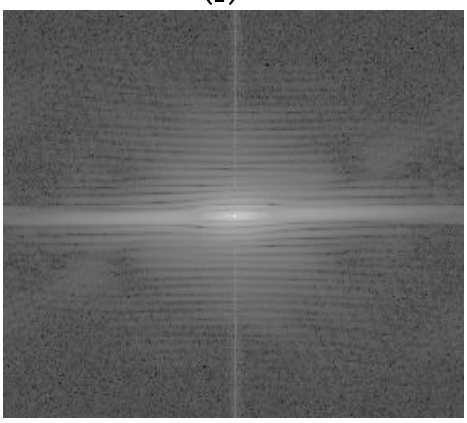

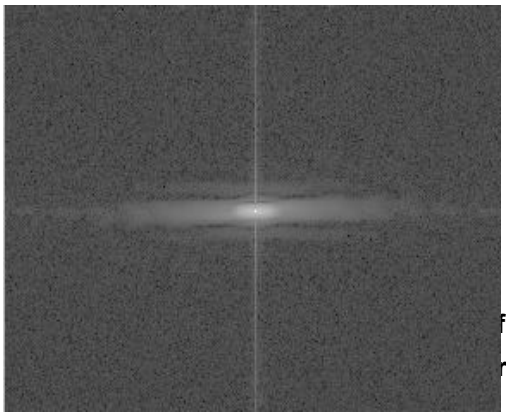

(h) (i)

**field in the period of temperature rise (b) Temperature field ration (c) Temperature field during tearing heat dissipation**

**(d) Radiation field in the period of temperature rise (e) Radiation field during complete penetration (f) Radiation field during tearing heat dissipation**

**(g) Spectrum in the period of temperature rise (h) Spectrum during complete penetration (i) Spectrum during tearing heat dissipation**

Complete the calculation of characteristic coefficient T, get the table of characteristic coefficient in frequency domain (Table 2) in each stage of belt tearing process.Draw the

line chart of characteristic coefficient T with respect to time, as shown in Fig. 9.

**Table 2: Frequency domain characteristic coefficient of conveyor belt tearing process**

| | Characteristic coefficient T | | | | |
|---|---|---|---|---|---|
| | Normal state (t1) | Temperature rising (t2) | Stopping penetration (t3) | Complete penetration (t4) | Heat dissipation (t5) |
| **Experiment 1** | 0.874~0.895 | 0.864~1.223 | 1.221~0.894 | 0.601~1.597 | 1.597↓ |
| **Experiment 2** | 0.826~0.863 | 0.859~1.248 | 1.247~0.872 | 0.658~1.584 | 1.584↓ |
| **Experiment 3** | 0.864~0.907 | 0.897~1.215 | 1.211~0.906 | 0.627~1.612 | 1.612↓ |

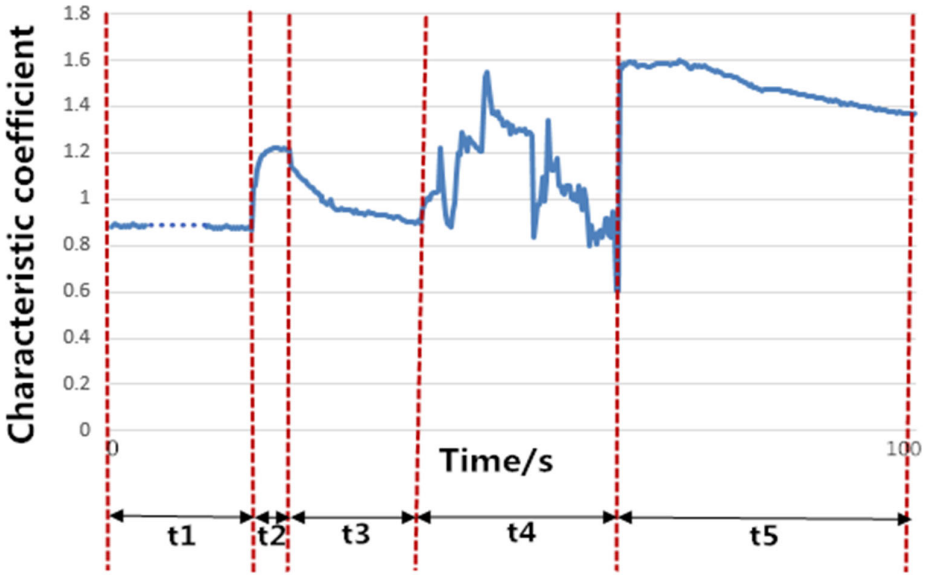


**Fig.9. Variation trend of frequency domain characteristic coefficient of infrared radiation field during belt tearing**

It can be seen from the Fig. 9 and Table 2 that the frequency domain characteristic coefficient of the conveyor belt is basically maintained at 0.8-0.9 during the period when the puncture point (t1) is not formed in the normal state of the conveyor belt. In the T2 period, T value increases slowly from 0.8 to 1.2 during the rise period of penetration temperature, which indicates that the conveyor belt has formed puncture point in the early stage of tearing that is not be pierced or torn yet. The gradient value of radiation transition region on the lower surface of conveyor belt increases gradually. The phenomenon of f(x,y) image in spatial domain is the separation of high radiation region from low radiation region. After stopping penetration, the frequency domain characteristic coefficient of (t3)

shows a decreasing trend, which indicates that the gradient value of radiation distribution of spatial domain image f (x,y) decreases gradually. Observing the characteristic coefficient of the complete penetration period (t4), T value fluctuates sharply from 0.6 to 1.6 during complete penetration period, because the surface temperature of exposed metal foreign body was much higher than that of the conveyor belt at the tear point, resulting in the radiation mean value of the whole thermal image, and the mean variance of radiation varied sharply with the degree of metal exposure. During the tearing heat dissipation period (t5), T value decreases slowly from 1.5 during the releasing period of tearing heat, which indicates that the gradient value of F (x, y) between the high and the low temperature transition region decreases slowly after tearing.Therefore, the fluctuation of the characteristic coefficient of infrared radiation field between 0.6 and 1.6 can be used as the precursor information of puncture characteristic information, i.e. tearing.

The experiments show that the ISAD method can identify and forewarn the tearing state of conveyor belt based on the spectrum distribution and characteristic coefficient of thermal radiation on the lower surface of conveyor belt during tearing process.The average processing time of single frame thermal image in three experiments is less than 30ms,which meets the requirements of on-line real-time detection of longitudinal tear of conveyor belt. In the coal mine working environment, there is more water and dust, which has a great impact on the equipment system using machine vision.Compared with the visual detection method of belt tearing proposed by Wang et al. [19], this method is not affected by the change of light intensity and the interference of dust and smoke on the visible light.In addition, Qiao and Liu [21] proposed a method for the tear detection of the conveyor belt according to the histogram of the infrared image. In this method, a longitudinal tear of the conveyor belt may be considered to exist if the grayscale value of the infrared image exceeds the threshold 170. Compared with the method proposed by Qiao, our method can also have a good detection accuracy under the condition of long-time working of conveyor belt.The main reason for this result may be that the grayscale value of the infrared image actually reflects the surface temperature of the conveyor belt. However, the surface temperature of the belt gradually increases with working time, which causes a change in the grayscale value of the infrared image. In other words, the potential tear of the belt is not the only factor that causes a change in the grayscale value of the infrared image. Thus, the fixed threshold of the infrared image results in a lower detection accuracy of the tear early-warning of the conveyor belt.

## 4. Conclusions

In this paper, a novel ISAD method is proposed for the longitudinal tear detection of conveyor belt for the first time in this field. By analyzing the radiation characteristics of target friction heating and background radiation characteristics, the authors select the appropriate 6-9 um spectral passband to obtain the maximum target background radiation contrast,which can improve the accuracy of analytical results and immunity to the environment.Infrared thermal imager captures the spatial domain image $f_t(\mathrm{x},\mathrm{y})$ of the lower surface of conveyor belt. $f_t(\mathrm{x},\mathrm{y})$ through two-dimensional FFT and frequency shift processing, the frequency domain characteristic coefficient T of infrared radiation field of spectrum image $F_t''(\mathrm{u},\mathrm{v})$ is obtained.The characteristic coefficient T can quantitatively describe the evolution characteristics of infrared radiation field and provide criterion for longitudinal tear detection.The experimental results not only demonstrate the performance

and effectiveness of our approaches, but also prove that the proposed method can meet the requirement of the real-time system.

## Conflicts of interest

The authors declare there is no conflict interest.

## Acknowledgments

This work is supported by the National Natural Science Foundation of China (Grant No.201601D01059) and Shanxi coal-based low-carbon joint fund (Grant No.U1810121) and Key Research and Development Plan for Industrial Science and Technology Jinzhong City, Shanxi Province，China (Grant No.201803D03111003) and High-end Foreign Expert Introduction Program (Grant No.G20190204013) and Scientific and Technologial Innovation Programs of Higher Education Institutions in Shanxi(Grand No.2019L0314)

## Reference

[1] D. He, Y. Pang, G. Lodewijks, Green operations of belt conveyors by means of speed control, Appl. Energy 188 (2017) 330-341.

[2] T.Z. Qiao, Y.F. Duan, B.Q. Jin, Infrared spectra imaging mechanism and modelling of the transport of hazard belt, Mater. Res. Innov. 19 (S6) (2015) 92-97.

[3] C. Wang, J. Zhang, The research on the monitoring system for conveyor belt based on pattern recognition, 1st Int. Conf. on Intelligent System and Applied Material (GSAM 2012), Taiyuan, 13–15 January (2012)622-625

[4] Y. Yang, C. Miao, X. Li, X. Mei, On-line conveyor belts inspection based on machine vision, Optik (Stuttg) 125 (2014) 5803-5807

[5] B. Yu, T. Qiao, H. Zhang, G. Yan, Dual band infrared detection method based on mid-infrared and long infrared vision for conveyor belts longitudinal tear,Measurement 120 (2018) 140-149

[6] Y. Pang, G. Lodewijks, A novel embedded conductive detection system for intelligent conveyor belt monitoring, Proc.IEEE Int.Conf.Serv.Oper.Logist.Informatics(2006) 803-808

[7] Q.L. Zeng, J.G. Wang, L. Wang, C.L. Wang, The research of coal mine conveyor belt tearing based on digital image processing, Proc. Int. Conf. Commun.Electron. Autom. Eng. (2013) 187-191

[8] T. Qiao, Y. Duan, Dynamic hazard of belt transport tracking and discerning method based on mean shift, Int. J. Min. Miner. Eng. 6 (2015) 309

[9] T. Qiao, B. Zhao, Infrared image detection of belt longitudinal tear based on SVM, J. Comput. Inf. Syst. 18 (2013) 7469-7475

[10] T. Qiao, Y. Tang, F. Ma, Real-time detection technology based on dynamic line edge for conveyor belt longitudinal tear, J. Comput. 8 (2013) 1065-1071

[11] J. Li, C. Miao, The conveyor belt longitudinal tear on-line detection based on improved SSR algorithm, Optik (Stuttg) 127 (2016) 8002-8010

[12] A. Harrison, B.C. Brown, Monitoring system for steel-reinforced conveyor belts,J. Eng. Ind. 108 (1986) 148-153

[13] J. Wang, C Miao, W. Wang, Research of X-ray nondestructive detector for high-speed running conveyor belt with steel wire ropes, Electronic Imaging and Multimedia Technology, November (2007) 12-15

[14] Y. Guan, J. Zhang, Y. Shang, Embedded sensor of forecast conveyer belt breaks, Fuzzy Systems and Knowledge Discovery, October (2008) 617-621

[15] F. Rong, C.Y. Miao, W. Xu, Development of X-ray non-destructive testing instrument for powerful conveyor belt, Precision Engineering,2011,19(10):2393-2401.

[16] J.Y. Qi, C. Tan, H. Li, Visual recognition of longitudinal rip of belt based on digital image processing, Coal Technology,2006,25(11 ):15-17

[17] J.Y. Qi, H.F. Yan, C. Tan, Research on machine vision detection system for conveyor belt tearing based on LABVIEW, Coal Engineering,2009(9):123-125

[18] J.Y. Qi, C. Tan, H. Li, Intelligent detection of conveyor belt longitudinal tear based on machine vision , Coal Mine Machinery,2006,27(11):110-111

[19] Z.X. Wang, T.Z. Qiao, Study and design on binocular vision on line monitoring system of conveyor belt longitudinal tearing, China Coal, 2018,44(4):87-90,105

[20] B.L. Zhao, T.Z. Qiao, Longitudinal tear detection method of conveyor belt based on support vector machine infrared image segmentation, Industry and Mine Automation,2014,40 (5),30-33

[21] T.Z. Qiao, W.L. Liu, Y.S. Pang, G.W. Yan, Research on visible light and infrared vision real-time detection system for conveyor belt longitudinal tea, Iet Science Measurement & Technology, 2016.9, 10(6):577-584

[22] T.Z. Qiao, L.L. Chen, Y.S. Pang, G.W. Yan, C.Y. Miao, Integrative binocular vision detection method based on infrared and visible light fusion for conveyor belts longitudinal tear, Measurement ,110 (2017) 192-201

[23] Y. Yang, C.C. Hou, T.Z. Qiao, H.T. Zhang, L. Ma, Longitudinal tear early-warning method for conveyor belt based on infrared vision, Measurement, 147 (2019)106817.

[24] Y. Zhang, Research on the arithmetic and application of zero value insulator identification based on infrared imaging, ChangSha: Hunan University,2013.

[25] B.P. Zou, Z.Y. Lou,J.X. Wang, G.T. Wang,L.S. Hu, Infrared thermography analysis of tunnel surrounding rock damage under blasting, Engineering Blasting, 2016,22(4):1-6.

[26] L.H. Yuan,J.F. Wang, Z.G. Zhu, M.J. Geng, Detection of material surface cracks by infrared thermal imaging microscope, Infrared Technology,2018,40(6):612-617.

[27] L. Qin, J.Y. Liu, J.L. Gong, Testing surface crack defects of sheet metal with ultrasonic lock-in thermography, Infrared and Laser Engineering, 2013, 42(5):1123-1130.

[28] F.Z. Feng, C.S. Zhang, Q.X. Min, Heating characteristics of metal plate crack in sonic IR imaging .Infrared and Laser Engineering, 2015, 44 (5):1456-1461.

[29] J.F. Zhu, Design of infrared detection system for conveyor belt tear of coal mine belt conveyor, New Industrialization, 17 (7) (2017)58-61

[30] M. Andrejiova, A. Grincova, D. Marasova, Measurement and simulation of impact wear damage to industrial conveyor belts,Wear 368-369 (2016) 400-407

[31] C.C. Hou, T.Z. Qiao, H.T. Zhang, Y.S. Pang, X.Y. Xiong, Multispectral visual detection method for conveyor belt longitudinal tear.Measurement ,143 (2019):246-257.

[32] H.M. Wang ,L. Lin , J. Cao, Visualization methods of the thermal field of high power LED lighting components, QingDao：IEEE/EI2010 Second IITA International Conference on Geoscience and Remote Sensing(2010)206-209.

[33] W.Q. An, C.Y. Wang, H. Sun, G.N. Pang, Selection and comparison of detection bands in infrared detection system, Journal of Changchun University of Technology (Natural Science Edition) 41(2) (2018)76-82

[34] Y.F. Wang, Application of MATLAB in Infrared Visualization Analysis, Infrared Technology, 26(3) (2004)65-68

[35] I. Bonnet, J. Gabelli, Probing Planck's law at home.European Journal of Physics, 2010(11):1463-1471

[36] Q. Zhang, H.J. Wang, Z. Wang, et al, Cutting characteristics and flash temperature analysis of pick coal and rock based on infrared thermal image detection, Journal of Sensing Technology, 29(5) (2016)686-692.

[37] H.R. Hua, L.H. Yuan, G.H. Wu, Quantitative detection of infrared thermal wave defects by transmission method, Infrared and Laser Engineering, 45(2) (2016)99-104.

[38] X. Wang, Z.W. Lu, Temperature monitoring and state analysis based on infrared thermal imaging technology, Coal Technology, 37(7) (2018)311-313.